Origin of electron-hole asymmetry in graphite and graphene

P. Plochocka,[1,2] P. Y. Solane,[1] R. J. Nicholas,[3] J. M. Schneider,[2] B. A. Piot,[2] D. K. Maude,[2]
O. Portugall,[1] and G. L. J. A. Rikken[1,2]

[1]*Laboratoire National des Champs Magnétiques Intenses, CNRS-UJF-UPS-INSA, 31400 Toulouse, France*
[2]*Laboratoire National des Champs Magnétiques Intenses, CNRS-UJF-UPS-INSA, 38042 Grenoble, France*
[3]*Clarendon Laboratory, Physics Department, Oxford University, Oxford OX1 3PU, United Kingdom*

(Received 10 November 2011; published 5 June 2012)

The electron-hole asymmetry has been measured in highly oriented pyrolitic graphite using magneto-optical absorption measurements. A splitting is observed for transitions at both the K point and the H point of the Brillouin zone of graphite where the effect of trigonal warping vanishes. This result is fully consistent with the Slonczewski, Weiss, and McClure Hamiltonian, providing the free-electron kinetic energy terms are included. Importantly, the free-electron terms enter via the Hamiltonian for an isolated carbon atom and provide a previously unsuspected source of electron-hole asymmetry in graphene.

DOI: 10.1103/PhysRevB.85.245410 PACS number(s): 71.20.−b, 71.70.Di, 78.67.Wj, 81.05.uf

I. INTRODUCTION

The electronic properties of graphite and graphene are inexorably intertwined. Graphite is a semimetal with small carrier pockets located along the HKH edge of the hexagonal Brillouin zone. Early attempts to calculate the band structure within a two-dimensional tight binding approach failed; graphite was predicted to be a gapless semiconductor with a linear dispersion where the bands touch.[1]

Today this result is understood to be the well-known band structure of graphene. Slonczewski and Weiss (SW), based on detailed group theoretical considerations, derived a Hamiltonian for graphite involving seven tight binding parameters, $\gamma_0, \ldots, \gamma_5, \Delta$.[2] In contrast to graphene, in graphite the interlayer coupling leads to an in-plane dispersion that depends on the momentum k_z parallel to the c axis. In a magnetic field the Slonczewski, Weiss, and McClure (SWM) Hamiltonian[3] has infinite order since the trigonal warping term γ_3 couples Landau levels with orbital quantum number n to Landau levels with quantum number $n+3$. Fortunately, the infinite Hamiltonian can be truncated and numerically diagonalized to find the eigenvalues.[4] At the H point the effect of γ_3 vanishes and the Landau-level energy spectrum depends only on γ_0. This is the origin of a widespread misconception in the literature, including our own work, that there is no electron-hole asymmetry at the H point.

Graphite has been extensively investigated,[5–19] in particular, magneto-optical techniques have been used to probe the energy spectrum at the H and K points where there is a joint maximum in the optical density of states.[20–25] Within the effective bilayer model[26] for graphite, with only two parameters, γ_0 and an effective interlayer coupling $2\gamma_1$, the observed splitting of the K-point transitions in the magnetoreflectance data was described by including the electron-hole asymmetry due to the nonvertical coupling term γ_4 phenomenologically.[23] Furthermore, the observed splitting of the H-point transitions was not assigned to electron-hole asymmetry as there is no trigonal warping at the H point, so the effect of γ_4 vanishes.[24]

In this article we extend our previous magneto-optical investigation of graphite to lower energies, lower temperatures, and higher magnetic fields. A splitting of both the H- and K-point transitions due to the electron-hole asymmetry is observed. This, at first sight, extremely surprising result, can be understood from the SWM Hamiltonian and originates from the often neglected free-electron kinetic energy terms that occur in the diagonal matrix elements.[4] When these terms are included, electron-hole asymmetry exists *for all values of* k_z. Importantly, the free-electron terms arise in the Hamiltonian for an isolated carbon atom providing a previously unsuspected source of electron-hole asymmetry in graphene.

II. SWM HAMILTONIAN

Starting from the SWM Hamiltonian (see the appendix) Nakao[4] derived an explicit form for the Landau-level energy spectrum at the H point, unfortunately neglecting, for simplicity, the small free-electron kinetic energy terms $\hbar^2k^2/2m$, where k is the in-plane wave vector and m is the *free*-electron mass. These terms are quantized in a magnetic field and their values are significant for all magnetic fields. The SWM Hamiltonian can easily be diagonalized at the H point and the correct expression for the Landau-level spectrum, including the free-electron terms, is

$$\begin{aligned} E^n_{3\pm} &= \frac{\Delta \pm \sqrt{(\Delta+\hbar^2 s/2m)^2 + 3ns\gamma_0^2a_0^2}}{2} + \frac{n\hbar^2 s}{2m}, \\ E^n_{1,2} &= \frac{\Delta \pm \sqrt{(\Delta-\hbar^2 s/2m)^2 + 3(n+1)s\gamma_0^2a_0^2}}{2} \\ &\quad + \frac{(n+1)\hbar^2 s}{2m}, \end{aligned} \tag{1}$$

where $n = 0,1,2,\ldots$, is the orbital quantum number, $s = 2eB/\hbar$, and $a_0 = 0.246$ nm. The Zeeman term has been omitted since it simply shifts the energies by $\pm g\mu_B B/2$ and can easily be added if required. At the H point the electron-hole asymmetry is provided by the free-electron term $n\hbar^2 s/2m$. Thus, the dipole-allowed transitions, $E^n_{3-} \rightarrow E^{n+1}_{3+}$ and $E^{n+1}_{3-} \rightarrow E^n_{3+}$, will be split by $\delta E = \hbar^2 s/m \simeq 0.23$ meV/T. Note that $\hbar^2 s/2m \ll s\gamma_0^2a_0^2$ so, to a very good approximation, $E^{n+1}_{3\pm} = E^n_{1,2}$, i.e., the Landau ladders remain doubly degenerate at the H point.

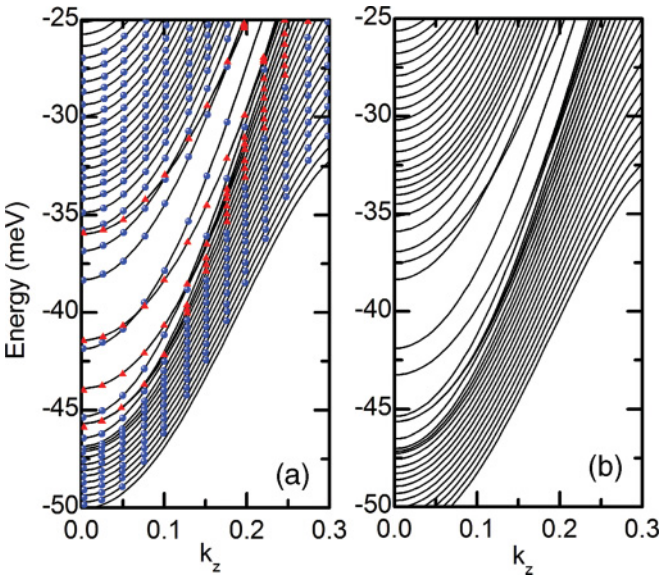

FIG. 1. (Color online) (a) Calculated Landau-level dispersion (solid lines) along k_z using the SWM parameters of Nakao[4] and including the free-electron terms. For comparison the calculated values of Nakao (symbols) are shown. (b) Calculated Landau-level dispersion along k_z neglecting the free-electron terms.

In a similar way, the bilayer expression[26] can be modified phenomenologically to include the free-electron term

$$E^n_{3\pm} = \pm\frac{1}{\sqrt{2}}[(\lambda\gamma_1)^2 + (2n+1)\varepsilon^2 - \sqrt{(\lambda\gamma_1)^4 + 2(2n+1)\varepsilon^2(\lambda\gamma_1)^2 + \varepsilon^4}]^{1/2} + \frac{\left(n+\frac{1}{2}\right)\hbar^2 s}{2m}, \quad (2)$$

where $n = 1,2,\ldots,\lambda = 2,\varepsilon = v_f\sqrt{2e\hbar B}$ is the characteristic magnetic energy, and $v_f = \sqrt{3}ea_0\gamma_0/2\hbar$ is the Fermi velocity. Equation (2) has not been derived explicitly; however, we have verified that the predicted behavior is in exact agreement with SWM with $\gamma_3,\ldots,\gamma_5,\Delta = 0$. Equally, the two special Landau levels (LL0 and LL-1) whose energy remains close to zero can be reproduced *within the bilayer approximation* using

$$E^n_{3\pm} = (n+3/2)\hbar^2 s/2m - (n+1)16(\hbar^2 s/2m)^2,$$

with $n = -1,0$.

Before presenting the experimental data, the importance of the free-electron kinetic energy terms is demonstrated by numerically diagonalizing the truncated 600×600 SWM matrix for a magnetic field $B = 0.3$ T using the SWM parameters of Nakao[4] to allow a comparison. The calculated Landau-level dispersion along k_z is shown in Fig. 1(a), including the free-electron terms. The symbols (circles and triangles) in Fig. 1(a) are taken from the calculations of Nakao at the same magnetic field (Fig. 3 of Ref. [4]). The triangles distinguish the triply degenerate Landau levels, which have a markedly different dispersion along k_z and correspond to leg orbits. Clearly there is perfect agreement between the two calculations. On the other hand, the calculations in Fig. 1(b) that neglect the free-electron terms significantly differ. Notably, the electron cyclotron energy is underestimated, while the hole cyclotron energy is overestimated. Thus, the free-electron terms have to be included in the SWM Hamiltonian if the correct energy spectrum is to be obtained. As our SWM calculations agree perfectly with the results of Nakao, we conclude that the free-electron terms were omitted from Eq. (9) of Ref. [4] but included in the numerical calculations of Nakao.

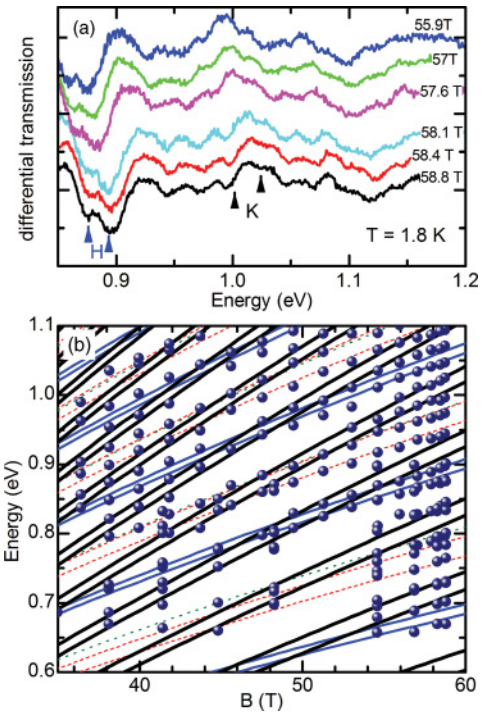

FIG. 2. (Color online) (a) Differential magnetotransmission spectra of graphite measured at magnetic fields in the range 55–59 T at $T \simeq 1.8$ K. (b) Magnetic-field dependence of the observed optical transitions in graphite. The calculated SWM energies of the transitions are shown as lines: H point $\Delta n = \pm 1$ (thin blue lines), "effective" H point $\Delta n = \pm 2$ (dashed red lines), $\Delta n = 0$ (dotted green lines), and K point $\Delta n = \pm 1$ (thick black lines).

III. MAGNETOABSORPTION

For the measurements, highly oriented pyrolitic graphite (HOPG) was exfoliated to produce mm size, $\simeq$20- to 40-nm-thick samples based on an estimated transmission of $\simeq$20%. Samples of different thickness give similar results that also agree with previous measurements on natural graphite.[24] The magnetotransmission measurements were performed in pulsed fields $\leqslant$60 T ($\simeq$400 ms). A tungsten halogen lamp provides a broad spectrum in the visible and near-infrared range and the absorption is measured in the Faraday configuration with the c axis of the graphite sample parallel to magnetic field. A nitrogen-cooled InGaAs photodiode array or an extended InGaAs detector analyzed the transmitted light dispersed by a spectrometer. The use of two detectors allows us to cover a wide energy range 0.6–1.1 eV. Differential transmission spectra were produced by normalizing all the acquired spectra by the zero-field transmission. Measurements to higher fields $\leqslant$150 T were performed using a semidestructive technique and pulse lengths of $\simeq$10 μs and the transmission of a polarized CO laser (0.229 eV) measured as a function of the magnetic field using a

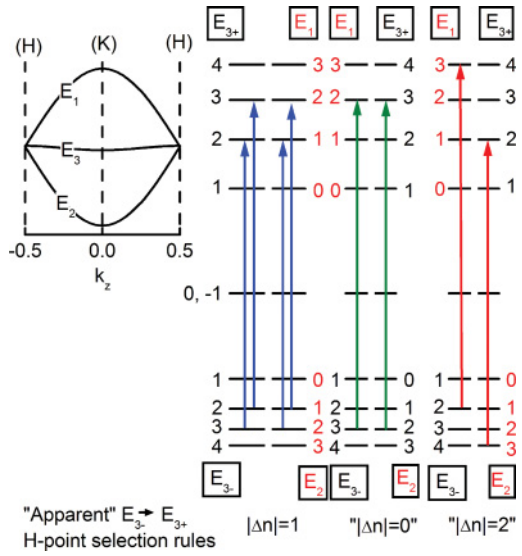

FIG. 3. (Color online) (left) Band structure of graphite along the HKH edge. (Right) Schematic of the Landau-level energies at the H point showing the electron-hole asymmetry. Arrows indicate dipole-allowed transitions ($\Delta n = \pm 1$). Transitions are labeled as "effective" $E_{3-} \rightarrow E_{3+}$ transitions with "apparent" dipole selection rules $\Delta n = \pm 1, 0, \pm 2$.

nitrogen-cooled HgCdTe photodiode coupled with a 200-MHz low-noise amplifier and an infrared tunable wave plate.

Representative differential absorption spectra measured at $T \simeq 1.8$ K in magnetic fields $B = 55$–59 T are shown in Fig. 2(a). The spectra contains a large number of lines reflecting the large number of K- and H-point transitions that cross in this energy region. Nevertheless, a clear splitting of the H-point and the K-point transitions is observed (arrows). The energy of the observed transitions are plotted as a function of magnetic field in Fig. 2(b). Before discussing these results, it is useful to consider the possible transitions at the H point. Dipole-allowed transitions have a change in the orbital quantum number of ± 1. Due to the doubly degenerate Landau-level spectrum at the H point with $E_{3\pm}^{n+1} = E_{1,2}^{n}$, there are a large number of allowed transitions between the valence band (E_{3-} or E_2) and the conduction band (E_{3+} or E_1). However, the understanding of the problem is greatly facilitated by the fact that all transitions involving bands E_2 or E_1 are degenerate with $E_{3-} \rightarrow E_{3+}$ transitions with "apparent" selection rules $\Delta n = 0$ and $\Delta n = \pm 2$. This is shown schematically in Fig. 3. The electron-hole asymmetry, also shown schematically here, splits both the $\Delta n = \pm 1$ and the $\Delta n = \pm 2$ transitions, while the $\Delta n = 0$ transitions remain unaffected. From Eq. (1) the splitting of the $\Delta n = \pm 2$ transitions is $\delta E = 2\hbar^2 s/m$, i.e., twice the size of the splitting of the $\Delta n = \pm 1$ transitions.

The energy of the observed H- and K-point transitions are plotted as a function of magnetic field in Fig. 2(b). As seen in the raw data, a splitting of the H-point and the K-point transitions is observed. The SWM transitions energies, calculated using the parameters in Table I, are indicated by the solid and dotted lines.

The energy of the H-point transitions depends only on $\gamma_0 = 3.15$ eV and the calculated splitting is independent of all other SWM parameters and vanishes only if the free-electron terms are not included in the Hamiltonian. We have verified that the predictions of Eq. (1) are exact. The observed splitting of the H-point $E_{3-}^{n(n+1)} \rightarrow E_{3+}^{n+1(n)}$ transitions (blue solid lines) is beautifully reproduced by the calculations. We stress that in either approach there are no fitting parameters; the size of the splitting is simply given by $\hbar^2 s/m \simeq 0.23$ meV/T. In addition, the observed splitting of the "effective" $E_{3-} \rightarrow E_{3+}$ transitions with "apparent" selection rules $\Delta n = \pm 2$ (dashed red lines) is twice as large, in agreement with the predictions for electron-hole asymmetry in Eq. (2).

TABLE I. Summary of the SWM parameters used.

$\gamma_0 = 3.15$ eV	$\gamma_1 = 0.37$ eV	$\gamma_2 = -0.0243$ eV
$\gamma_3 = 0.31$ eV	$\gamma_4 = 0.07$ eV	$\gamma_5 = 0.05$ eV
$\Delta = -0.002$ eV		

The calculated splitting of the K-point transitions depends on the SWM parameters used, notably γ_4 and γ_5. We adjust very slightly $\gamma_1 = 0.37$ eV to fit the observed transitions (slope of the magnetic-field dependence) and use the accepted values for the other SWM parameters that are summarized in Table I. The agreement turns out to be very good, making a further refinement of the parameters unnecessary. A comparison of the SWM splitting $\simeq$23 meV at $B = 60$ T with $\hbar s/m \simeq 14$ meV suggests that γ_4 and γ_5 are responsible for approximately 40% of the splitting. The relative importance of the contribution of the free-electron kinetic energy terms to the electron-hole asymmetry means that any data analysis that neglects them would lead to a significant over estimation of size of γ_4 or γ_5.

Polarization-resolved magnetotransmission, in fields up to ± 140 T are shown in Fig. 4(a). Mainly K-point transitions are observed in this energy range. The different field directions corresponds to different polarizations and the features are shifted in field due to the different energy of the $n \rightarrow n+1$ and $n+1 \rightarrow n$ transitions. The feature around 100 T is the fundamental $0 \rightarrow 1$ transition, which should not be split (shifted) since the LL0 is special and has a free-electron

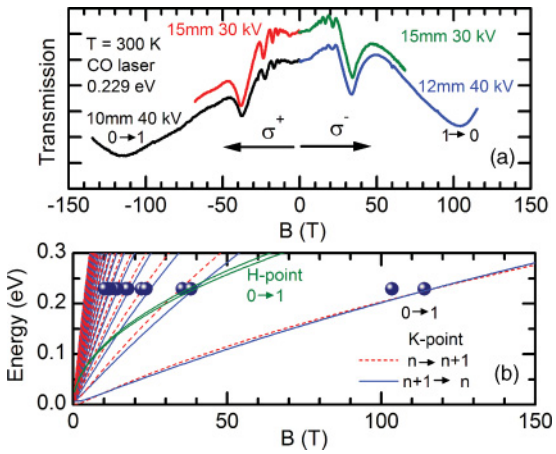

FIG. 4. (Color online) (a) Magnetotransmission of graphite showing mainly K-point transitions. (b) Calculated SWM transitions together with the measured splitting (symbols). There is no electron-hole asymmetry for the $0 \rightarrow 1$ K-point transition that splits due to the Zeeman term.

term $\simeq(n+3/2)\hbar^2 s/2m$ with $n=0$ which is identical to the free-electron term of the $n=1$ Landau level $(n+1/2)\hbar^2 s/2m$. The SWM prediction for the transitions are shown in Fig. 4(b) together with the measured field splitting. It can be seen that there is indeed no effect of electron-hole asymmetry for the calculated $0\rightarrow 1$ K-point transition (solid and broken lines). Nevertheless, the measured position is shifted by $\simeq$10 T between the two polarizations. An enhanced spin splitting of the 0 Landau level (lowering of the energy of the full spin level due to exchange) could give rise to a measurable electron-hole asymmetry, shifting one of the transitions to lower magnetic field [as observed in Fig. 4(b)] when filling effects are taken into account.[10,27]

IV. CONCLUSION

We have measured the electron-hole asymmetry in HOPG using magneto-optical absorption measurements. A splitting is observed for transitions at both the K point and the H point of the Brillouin zone of graphite where the effect of trigonal warping vanishes. This, at first sight, surprising result is fully consistent with the SWM Hamiltonian, providing the free-electron kinetic energy terms are included. The free-electron terms arise in the Hamiltonian of an isolated carbon atom (the basic building block of the SWM Hamiltonian). We have shown that the free-electron terms lead to a significant electron-hole asymmetry correcting a long-standing erroneous assumption found throughout the literature (including our own work) that since the effect of γ_3, the SWM trigonal warping parameter vanishes at the H point, there is no electron-hole asymmetry at the H point in graphite.

Finally, we note that the free-electron terms enter the Hamiltonian of both graphite and graphene via the Hamiltonian of an isolated carbon atom.[1,2] Moreover, the Landau-level energy spectrum of graphene in the vicinity of the Dirac point can be derived from the SWM Hamiltonian simply by setting all the interlayer coupling parameters $\gamma_1,\ldots,\gamma_5=0$. The analytic solution of this simplified Hamiltonian is nothing other than Eq. (1). Thus, the free-electron terms provide a previously unsuspected origin for the observed electron-hole asymmetry in graphene.[28]

ACKNOWLEDGMENTS

We thank Mark Goerbig for theoretical advice. This work was partially supported by EuroMagNET II under the EU Contract No. 228043.

APPENDIX: SWM HAMILTONIAN

We include here for completeness the magnetic Hamiltonian for graphite, following the notation of Nakao.[4] The SW Hamiltonian, which is based on a Taylor expansion of the full tight binding Hamiltonian (valid close to the HKH edge of the Brillouin zone) is given by[2,4]

$$H_{\mathrm{SW}}=\begin{pmatrix} E_1+\frac{\hbar^2k^2}{2m} & 0 & \sigma_- k_+ & \sigma_- k_- \\ 0 & E_2+\frac{\hbar^2k^2}{2m} & -\sigma_+ k_+ & \sigma_+ k_- \\ \sigma_- k_- & -\sigma_+ k_- & E_3+\frac{\hbar^2k^2}{2m} & \frac{\sqrt{3}}{2}\gamma_3\Gamma k_+ \\ \sigma_- k_+ & \sigma_+ k_+ & \frac{\sqrt{3}}{2}\gamma_3\Gamma k_- & E_3+\frac{\hbar^2k^2}{2m} \end{pmatrix},$$

with

$$\begin{aligned} E_1 &= \Delta+\gamma_1\Gamma+\frac{1}{2}\gamma_5\Gamma^2 \\ E_2 &= \Delta-\gamma_1\Gamma+\frac{1}{2}\gamma_5\Gamma^2 \\ E_3 &= +\frac{1}{2}\gamma_2\Gamma^2 \end{aligned} \tag{A1}$$

where $\sigma_\pm=-(a_0\sqrt{6}/4)(\gamma_0\pm\gamma_4\Gamma)$, $\Gamma=2\cos(\pi\xi)$, $\xi=c_0k_z/2\pi$, a_0, and c_0 are lattice constants and the wave vector $k_\pm=k_x\pm ik_y$ is measured from the HKH zone edge. Note that for $\Gamma=0$, which occurs at the H point ($k_z=\pm\pi/c_0$), the effect of the trigonal warping parameter γ_3 vanishes.

A magnetic field was introduced by McClure[3] using the usual Peierls substitution $\boldsymbol{k}\rightarrow\boldsymbol{k}+e\boldsymbol{A}/\hbar$.[29] Here we use the Landau gauge $\boldsymbol{A}=(0,Bx,0)$ for a magnetic field along the z direction. Physical insight is facilitated if we write the magnetic Hamiltonian of McClure using annihilation and creation operators $a=\sqrt{s}k_-$ and $a^\dagger=\sqrt{s}k_+$, where $k_\pm\rightarrow k_x\pm i(k_y+eBx/\hbar)$ and $s=\sqrt{2eB/\hbar}$. Making this substitution we obtain as a first step

$$H'=\begin{bmatrix} E_1+\frac{\hbar^2 s}{2m}(a^\dagger a+\frac{1}{2}) & 0 & \sigma_-\sqrt{s}a^\dagger & \sigma_-\sqrt{s}a \\ 0 & E_2+\frac{\hbar^2 s}{2m}(a^\dagger a+\frac{1}{2}) & -\sigma_+\sqrt{s}a^\dagger & \sigma_+\sqrt{s}a \\ \sigma_-\sqrt{s}a & -\sigma_+\sqrt{s}a & E_3+\frac{\hbar^2 s}{2m}(a^\dagger a+\frac{1}{2}) & \frac{\sqrt{3}\gamma_3\Gamma}{2}\sqrt{s}a^\dagger \\ \sigma_-\sqrt{s}a^\dagger & \sigma_+\sqrt{s}a^\dagger & \frac{\sqrt{3}\gamma_3\Gamma}{2}\sqrt{s}a & E_3+\frac{\hbar^2 s}{2m}(a^\dagger a+\frac{1}{2}) \end{bmatrix}.$$

For the linear harmonic oscillator wave function ϕ_n, a and $a^\dagger$ satisfy the usual relations, $a\phi_n=\sqrt{n}\phi_{n-1}$, $a^\dagger\phi_n=\sqrt{n+1}\phi_{n+1}$, and $[a,a^\dagger]=1$. Applying these rules and using the basis set $\varphi(n)=(\phi_n,\phi_n,\phi_{n-1},\phi_{n+1})$, it is trivial to derive an expression for $H'\varphi(n)$. The terms with γ_3 couple the levels ϕ_{n-1} to ϕ_{n+2} and ϕ_{n+1} to ϕ_{n-2}. Due to the coupling it is not possible to obtain the Landau-level energies simply by diagonalizing the 4×4 matrix H'. Instead, the magnetic Hamiltonian has infinite order. Using

the notation of Nakao,

$$H_{\mathrm{SWM}} = \begin{pmatrix} D_0(-1) & O & O & D_1(-1) & O & \dots \\ O & D_0(0) & O & O & D_1(0) & \dots \\ O & O & D_0(1) & O & O & \dots \\ D_1^{\dagger}(-1) & O & O & D_0(2) & O & \dots \\ O & D_1^{\dagger}(0) & O & O & D_0(3) & \dots \\ . & . & . & . & . & . \\ . & . & . & . & . & . \\ . & . & . & . & . & . \end{pmatrix},$$

where O is a 4×4 zero matrix and the other matrices and are obtained from the transpose of $H'\varphi(n)$ by excluding the γ_3 terms $[D_0(n)]$ or including only the γ_3 terms $[D_1(n), D_1^{\dagger}(n)]$ as appropriate. Operating with H' on the basis set $\varphi(n)$ it is easy to show that,

$$D_0(n) = \begin{bmatrix} E_1 + \frac{\hbar^2 s}{2m}(n+\frac{1}{2}) & 0 & \sigma_-\sqrt{ns} & \sigma_-\sqrt{(n+1)s} \\ 0 & E_2 + \frac{\hbar^2 s}{2m}(n+\frac{1}{2}) & -\sigma_+\sqrt{ns} & \sigma_+\sqrt{(n+1)s} \\ \sigma_-\sqrt{ns} & -\sigma_+\sqrt{ns} & E_3 + \frac{\hbar^2 s}{2m}(n-\frac{1}{2}) & 0 \\ \sigma_-\sqrt{(n+1)s} & \sigma_+\sqrt{(n+1)s} & 0 & E_3 + \frac{\hbar^2 s}{2m}(n+\frac{3}{2}) \end{bmatrix},$$

$$D_1(n) = \begin{pmatrix} 0 & 0 & 0 & 0 \\ 0 & 0 & 0 & 0 \\ 0 & 0 & 0 & 0 \\ 0 & 0 & \frac{\sqrt{3}\gamma_3\Gamma}{2}\sqrt{(n+2)s} & 0 \end{pmatrix}.$$

The full basis set is now $\psi = [\varphi(-1),\varphi(0),\varphi(1),\varphi(2), \dots,]$ and it is easy to verify that $H_{\mathrm{SWM}}\psi$ correctly reproduces the observed coupling when operating on ϕ_n with H'. It is important to exclude from $D_0(-1)$ and $D_0(0)$ terms corresponding to negative quantum numbers of ϕ_n to avoid coupling to levels that physically do not exist.

At the H point, $\Gamma = 0$ so the γ_3 matrix elements vanish and the Landau levels can be obtained simply by diagonalizing the 4×4 matrix $D_0(n)$. The analytic expressions for the Landau levels at the H point are given in Eq. (1). Away from the H point, the infinite matrix H_{SWM} has to be truncated and numerical techniques used to find the eigenvalues.

[1] P. R. Wallace, Phys. Rev. **71**, 622 (1947).
[2] J. C. Slonczewski and P. R. Weiss, Phys. Rev. **109**, 272 (1958).
[3] J. W. McClure, Phys. Rev. **119**, 606 (1960).
[4] K. Nakao, J. Phys. Soc. Jpn. **40**, 761 (1976).
[5] D. E. Soule, J. W. McClure, and L. B. Smith, Phys. Rev. **134**, A453 (1964).
[6] S. J. Williamson, S. Foner, and M. S. Dresselhaus, Phys. Rev. **140**, A1429 (1965).
[7] P. R. Schroeder, M. S. Dresselhaus, and A. Javan, Phys. Rev. Lett. **20**, 1292 (1968).
[8] J. A. Woollam, Phys. Rev. Lett. **70**, 811 (1970).
[9] J. A. Woollam, Phys. Rev. B **4**, 3393 (1971).
[10] Y. Shimamoto, N. Miura, and H. Nojiri, J. Phys.: Condens. Matter **10**, 11289 (1998).
[11] I. A. Luk'yanchuk and Y. Kopelevich, Phys. Rev. Lett. **93**, 166402 (2004).
[12] I. A. Luk'yanchuk and Y. Kopelevich, Phys. Rev. Lett. **97**, 256801 (2006).
[13] G. P. Mikitik and Yu. V. Sharlai, Phys. Rev. B **73**, 235112 (2006).
[14] J. M. Schneider, M. Orlita, M. Potemski, and D. K. Maude, Phys. Rev. Lett. **102**, 166403 (2009).
[15] Z. Zhu, H. Yang, B. Fauqué, Y. Kopelevich, and K. Behnia, Nat. Phys. **6**, 26 (2009).
[16] J. M. Schneider, N. A. Goncharuk, P. Vasek, P. Svoboda, Z. Vyborny, L. Smrcka, M. Orlita, M. Potemski, and D. K. Maude, Phys. Rev. B **81**, 195204 (2010).
[17] I. A. Luk'yanchuk and Y. Kopelevich, Phys. Rev. Lett. **104**, 119701 (2010).
[18] J. M. Schneider, M. Orlita, M. Potemski, and D. K. Maude, Phys. Rev. Lett. **104**, 119702 (2010).
[19] S. B. Hubbard, T. J. Kershaw, A. Usher, A. K. Savchenko, and A. Shytov, Phys. Rev. B **83**, 035122 (2011).
[20] R. E. Doezema, W. R. Datars, H. Schaber, and A. Van Schyndel, Phys. Rev. B **19**, 4224 (1979).
[21] M. Orlita, C. Faugeras, G. Martinez, D. K. Maude, M. L. Sadowski, and M. Potemski, Phys. Rev. Lett. **100**, 136403 (2008).
[22] M. Orlita, C. Faugeras, J. M. Schneider, G. Martinez, D. K. Maude, and M. Potemski, Phys. Rev. Lett. **102**, 166401 (2009).
[23] K.-C. Chuang, A. M. R. Baker, and R. J. Nicholas, Phys. Rev. B **80**, 161410 (2009).
[24] N. Ubrig, P. Plochocka, P. Kossacki, M. Orlita, D. K. Maude, O. Portugall, and G. L. J. A. Rikken, Phys. Rev. B **83**, 073401 (2011).
[25] L.-C. Tung, P. Cadden-Zimansky, J. Qi, Z. Jiang, and D. Smirnov, Phys. Rev. B **84**, 153405 (2011).
[26] M. Koshino and T. Ando, Phys. Rev. B **77**, 115313 (2008).
[27] Y. Takada and H. Goto, J. Phys.: Condens. Matter **10**, 11315 (1998).
[28] R. S. Deacon, K.-C. Chuang, R. J. Nicholas, K. S. Novoselov, and A. K. Geim, Phys. Rev. B **76**, 081406 (2007).
[29] J. M. Luttinger and W. Kohn, Phys. Rev. **97**, 869 (1955).